Journal of Social Research
P-ISSN: 2827-9832
E-ISSN: 2828-335x
http://ijsr.internationaljournallabs.com/index.php/ijsr

ALLOY CRYSTAL STRUCTURE AND VOLUMETRIC MASS DENSITY ANALYSIS

D Tamara Dirasutisna[1*], Bintang Adjiantoro[2], Sarinah Sihombing[3***], Muhammad Rifni[4****], Ruddy Max Damara Gugat[5*****]**

[1,2,3,4,5]*Universitas Indonesia*

[*] *PapaTamaraAugust@gmail.com* [**] *bintangadjiantoro11@yahoo.com* [***] *P3m@itltrisakti.ac.id*

[****] *rifnim@gmail.com* [*****] *rudydamara.itl@gmail.com*

ABSTRACT

Volumetric mass density and changes in crystal structure analysis of Sn-xBi alloy and Sn-xBi-yAl alloys have been conducted to enhance our understanding of these materials. The Sn-xBi alloy, with various compositions including Sn-0Bi, Sn-10Bi, Sn-30Bi, Sn-52Bi, and Sn-70Bi, and the Sn-xBi-yAl alloys, with compositions including Sn-52Bi-0.05Al, Sn-52Bi-0.11Al, Sn-52Bi-0.14Al, Sn-52Bi-0.19Al, and Sn-52Bi-0.25Al, were synthesized for this research. The selection of Sn-xBi-yAl compositions was based on the optimal composition of Sn-xBi alloys, specifically Sn-52Bi, which possesses the lowest melting point at 142.8°C. The determination of melting points was carried out using the Differential Scanning Calorimetry (DSC) method. Crystal structure characterization was accomplished using X-ray diffraction (XRD) techniques, with subsequent analysis performed through the Generalized Structure Analysis System (GSAS) method. These investigations are pivotal as they provide insights into the material properties and structural changes in Sn-xBi and Sn-xBi-yAl alloys, which have significant implications in various industrial applications and technological advancements. The results of this research are expected to contribute to the optimization of these alloy systems, leading to improved performance and potential innovations in materials science and engineering.

Keywords: *composition, melting point, GSAS (Generalized structure Analysis System)*

INTRODUCTION

Crystallography, the branch of science that studies the atomic and molecular structure of crystals, has been an important foundation in our understanding of the properties of solid materials. In this context, research on “Crystal Structure of Alloys and Volumetric Mass Density Analysis” plays a central role in delving deeper into the secrets of material structure and revealing its critical properties in various applications. This research examines the characteristics of alloy materials as well as analyzes their volumetric mass density with the aim of providing better insight into the material properties that influence performance in various contexts, such as industry, technology, and natural science (Lesyk et al., 2021).

As evidence of the importance of understanding the crystal structure of alloys, Smith et al. (2020) explain, "A deep understanding of atomic interactions in alloy crystals is the key to optimizing material properties and creating materials with tailored performance."

Galera-Rueda et al. (2021) underscored the relevance of volumetric mass density analysis by stating, “The study of volumetric mass density in the crystal structures of alloys has helped identify correlations between atomic arrangement and mechanical properties of materials, paving the way for the development of high-tech materials.” Research by Feather et al. (2019) highlights the importance of alloy diversity and emphasizes, "In the era of globalization, better understanding of the crystal structure of alloys from various natural resources is key to sustainable resource and industrial development." In an industrial context, research by (Ruiz-

Esparza-Rodríguez et al., 2021) stated, "Optimization of the crystal structure of alloys in critical industrial components has helped reduce production costs and increase the efficiency of manufacturing processes."

By looking at the valuable contributions of previous research in the understanding of alloy crystal structure and volumetric mass density analysis, this research seeks to continue this legacy of knowledge by delving deeper and expanding our understanding of the properties of alloy materials (Liang et al., 2020; Oakwood et al., 2002). In this context, this research has important relevance in supporting the development of industry, technology, and science, as well as promoting the use of Indonesia's natural resources more effectively and sustainably.

METHOD

Research carried out synthetic for the composition Sn-0Bi, Sn-10Bi, Sn-30Bi, Sn-52Bi, and Sn-70Bi. Furthermore, an optimum composition was taken from the five compositions from the five compositions to make a new composition with the addition of aluminum in five various compositions specifically Sn-xBi-yAl in five varied compositions for constant x and changing y. The volumetric mass density measurements were done through three steps. The first step was done through a theoretical approach using standard volumetric mass density as the basis. The second step was done by using a tool called a densitometer and, the third as the final step is using GSAS (General Structure Analysis System) method analysis (Nishikawa et al., 2006; Parakh et al., 2021).

To measure volumetric mass density using calculations as the basis, the following formulas are used:

$$\rho_{Sn-Bi} = \frac{v_{Sn}}{\left(v_{Sn}+v_{Bi}\right)}\rho_{Sn} + \frac{v_{Bi}}{\left(v_{Sn}+v_{Bi}\right)}\rho_{Bi} \quad \text{.....(1)}$$

And

$$\rho_{Sn-Bi-Al} = \frac{v_{Sn}}{\left(v_{Sn}+v_{Bi}+v_{Al}\right)}\rho_{Sn} + \frac{v_{Bi}}{\left(v_{Sn}+v_{Bi}+v_{Al}\right)}\rho_{Bi} + \frac{v_{Al}}{\left(v_{Sn}+v_{Bi}+v_{Al}\right)}\rho_{Al} \quad \text{.....(2)}$$

Where :

ρ_{Sn-Bi} = Sn-Bi alloy volumetric mass density (gram/cm^3)

$\rho_{Sn-Bi-Al}$ = Sn-Bi-Al volumetric mass density (gram/cm^3)

ρ_{Sn} = Sn volumetric mass density (gram/cm^3)

ρ_{Bi} = Bi volumetric mass density (gram/cm^3)

ρ_{Al} = Al volumetric mass density (gram/cm^3)

v_{Sn} = Sn element volume (cm^3)

v_{Bi} = Bi element volume (cm^3)

v_{Al} = Al element volume (cm^3)

As to calculate volumetric mass density using direct measurement, the following formula was used:

$$\rho = \frac{M_{udara}}{\left(M_{udara}-M_{z.cair}\right)}\rho_{z.cair} \quad \text{.....(3)}$$

Where :

ρ = Volumetric mass density being measured (gram/cm^3)

$\rho_{z.cair}$ = Liquid substance volumetric mass density (gram/cm^3)

M_{ud} = Object mass in the air (gram)

$M_{z.cair}$ = Object mass in liquid substance (gram)

RESULTS AND DISCUSSION

The result of the measurement and calculation can be seen on the following table:

Table 1. Volumetric Mass Density from Measurement and Calculation

Sample	Sn Mass	Bi Mass	Al Mass	□(Calc.)	□(Meas.)	Dev.
	Gram	gram	gram	gram/cc	gram/cc	%
Sn-0Bi	20,6	0	-	7,310	7,430	1,6416
Sn-10Bi	17,94	2,1	-	7,509	7,490	-0,2530
Sn-30Bi	14,7	6,1	-	7,908	7,810	-1,2393
Sn-52Bi	9,6	10,42	-	8,416	7,820	-7,0817
Sn-70Bi	6,04	14,08	-	8,879	8,920	0,4618
Sn-52Bi-0,05Al	3,6999	4,0082	0,001	8,4205	8,3640	-0,670982
Sn-52Bi-0,11Al	3,6955	4,0035	0,0023	8,4175	8,4266	0,1081081
Sn-52Bi-0,14Al	3,6926	4,0001	0,003	8,4159	8,3681	-0,567973
Sn-52Bi-0,19Al	3,6882	3,9955	0,004	8,4136	8,0090	-4,808881
Sn-52Bi-0,25Al	3,6855	3,9926	0,51	8,4110	8,2028	-2,47533

The generated volumetric mass density for the Sn-xBi alloys, whether generated from calculation based on standard volumetric mass density of each element or direct measurement, both have increased volumetric mass density value. The standard volumetric density of Sn (Tin) is $\rho_{Sn} = 7{,}31\, gram/cc$ (Lee) and of Bi (Bismuth) is $\rho_{Bi} = 9{,}78\, gram/cc$ (Lee) (Shtender et al., 2020).

By using the XRD method, the grid parameters and crystal structures were obtained. The results were analyzed using the GSAS (*General Structure Analysis System*) program and the method that was used was the *Rietveld* method. This method function to compare standard parameter and measurement parameter (Anderson et al., 2001; Andrade et al., 2023; Kim et al., 2000). With this method, the changes in the parameter can be known, such as the changes in the lattice constants, volumes, phases, and volumetric mass density, for example.

The analysis result of the GSAS (***General Structure Analysis System***) can be seen in Table 2 as follows:

Table.2.Sn-xBi and Sn-xBi-yAl Rietveld Method Refinement Result

Sample		a=b Å	c Å	Volume (Å^3)	Vol(tot) (Å^3)	ρ Gram/cc	ρ Gram/cc	Crystal System
Sn-0Bi	Sn	5,834	3,188	108,501	1102,937	7,321	7,321	Tetragonal
Sn-10Bi	Sn	5,845	3,187	108,877		7,242		Tetragonal
	Bi	4,532	11,845	243,310	425,377	9,882	7,506	Hexagonal

Sample		a=b Å	c Å	Volume (Å³)	Vol(tot) (Å³)	ρ Gram/cc	ρ Gram/cc	Crystal System
Sn-30Bi	Sn	5,845	3,186	108,853	397,890	7,243		Tetragonal
	Bi	4,534	11,849	243,530		9,897	8,039	Hexagonal
Sn-52Bi	Sn	5,822	3,178	107,725	369,665	7,318		Tetragonal
	Bi	4,537	11,857	244,021		9,852	8,636	Hexagonal
Sn-70Bi	Sn	5,845	3,187	108,856	351,607	7,242		Tetragonal
	Bi	4,533	11,856	243,642		9,868	9,080	Hexagonal
Sn-52Bi-0,05Al	Sn	5,847	3,187	108,923		7,238		Tetragonal
	Bi	4,542	11,871	280,133	455,059	9,982		Hexagonal
							8,271	
	Al	4,041	4,041	66,003		2,715		FCC
Sn-52Bi-0,11Al	Sn	5,853	3,189	109,236		7,217		Tetragonal
	Bi	4,540	11,867	279,971	455,210	9,828	8,170	Hexagonal
	Al	4,041	4,041	66,003		2,715		FCC
Sn-52Bi-0,14Al	Sn	5,845	3,185	108,805		7,246		Tetragonal
	Bi	4,453	11,865	274,541	449,031	9,818	8,158	Hexagonal
	Al	4,035	4,035	65,685		2,728		FCC
Sn-52Bi-0,19Al	Sn	5,847	3,186	108,927		7,237		Tetragonal
	Bi	4,541	11,870	280,085	455,560	9,822	8,163	Hexagonal
	Al	4,052	4,052	66,548		2,693		FCC
Sn-52Bi-0,25Al	Sn	5,820	3,175	107,530		7,331		Tetragonal
	Bi	4,596	12,200	291,320	464,535	9,471	8,022	Hexagonal
	Al	4,035	4,035	65,685		2,728		FCC

Table 2 shows changes in lattice constants, volumes, and volumetric mass densities. For Sn-xBi alloys, raises in volumetric density values occurred with the increments in the Bi element. As for the Sn-52Bi-Al, raises and decreases occurred (further research is needed) (Moon et al., 2000; Tong et al., 2022).

A direct measurement using the densitometer tool to measure volumetric mass density was done with the GSAS (***General Structure Analysis System***) method analysis, as a comparison to the measurement that was done using the theoretical calculation based on the volumetric mass density of each element (Choi & Lee, 2000; Zhou et al., 2009).

The following is the comparison of the three measurements:

Table.3. Comparison of the three measurement methods of Sn-xBi and Sn-xBi-yAl alloys volumetric mass density

Sample	ρ(Calc.) gram/cc	ρ(Meas.) gram/cc	ρ(GSAS) gram/cc	Dev(*&**) %	Dev(*&@) %
Sn-0Bi	7,31	7,43	7,321	1,642	0,150
Sn-10Bi	7,509	7,49	7,506	-0,253	-0,040
Sn-30Bi	7,908	7,81	8,039	-1,239	1,657
Sn-52Bi	8,416	7,82	8,636	-7,082	2,614
Sn-70Bi	8,879	8,92	9,08	0,462	2,264
Sn-52Bi-0,05Al	8,4205	8,364	8,271	-0,671	-1,775

Sn-52Bi-0,11Al	8,4175	8,4266	8,17	0,108	-2,940
Sn-52Bi-0,14Al	8,4159	8,3681	8,158	-0,568	-3,064
Sn-52Bi-0,19Al	8,4136	8,009	8,163	-4,809	-2,979
Sn-52Bi-0,25Al	8,411	8,2028	8,022	-2,475	-4,625

Notes :
Dev(*&**)= Volumetric mass density deviation between standard calculation and direct measurement
Dev(*&**)= Volumetric mass density deviation between standard calculation and *Rietveld* method

The following is the function graph of Sn-xBi alloy based on calculation, direct measurement, and refinement using the *Rietveld* method.

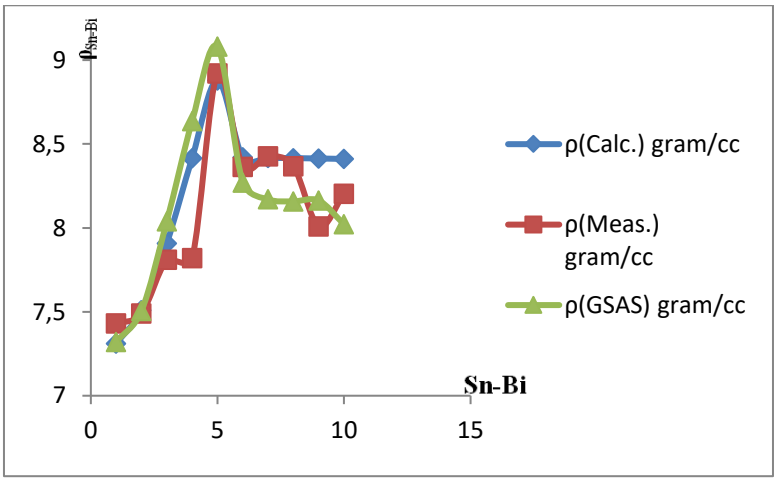

Graph.1.Sn-xBi Volumetric Mass Density Graph

The following is the Determination Coefficient (R^2) and Correlation Coefficient [R] of Sn-xBi volumetric mass density table

Table 4. Sn-xBi Determination Coefficient and Correlation Coefficient

Parameter	**R^2**	**R**	**Equation**
ρ(Calc.)	0,996	0,998	y = 0,045x2 + 0,131x + 7,109
ρ(Meas.)	0,961	0,980	y = 0,069x3 - 0,496x2 + 1,204x + 6,624
ρ(GSAS)	0,988	0,994	y = 0,041x2 + 0,215x + 7,013

The following is the function graph of Sn-52Bi-yAl based on calculation, direct measurement, and refinement using the *Rietveld* method.

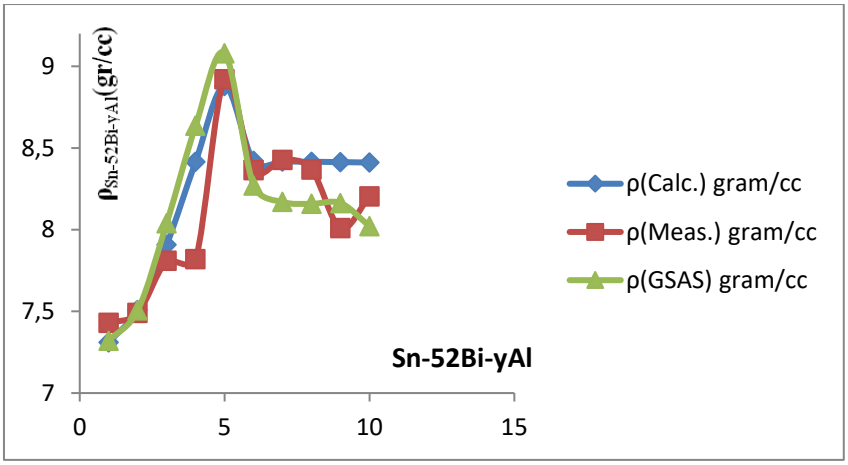

Graph.2. Sn-52Bi-yAl Volumetric Mass Density Graph

The following is the Determination Coefficient table (R^2) and Correlation Coefficient [R] of the Sn-52Bi-yAl table:

Table.5.Sn-52Bi-yAl Determination Coefficient and Correlation Coefficient

Parameter	R^2	R	Equation
ρ(Perhit)	0,998	0,999	y = -0,000x3 + 0,001x2 - 0,005x + 8,425
ρ(Peng.)	0,868	0,932	y = 0,056x3 - 0,508x2 + 1,267x + 7,533
ρ(GSAS)	0,996	0,998	y = -0,019x3 + 0,171x2 - 0,485x + 8,605

CONCLUSION

For the Sn-xBi alloys, a rise in volumetric mass density happened, whether the analysis was using calculation, direct measurement, or the Rietveld refining method. As for the Sn-52bi-yAl, a decrease in rise and decreases in volumetric mass density happened (there is a possibility that another element got in the melting process). The analysis result can be considered as successful because the deviation between the results obtained through direct measurement and standard volumetric mass density is quite small, and likewise for the measurement analysis between the Rietveld refining method and the calculation based on standard volumetric mass density.

Table.3. shows changes in the lattice constants, volume, and volumetric mass density for each alloy but, without changing the crystal structure of each element (Table.2.). Based on the Determination Coefficient and Correlation Coefficient values, the result of the analysis using the Rietveld refining method are better than that of using direct measurement (see Table.4. and Table.5.).

REFERENCES

Anderson, I. E., Foley, J. C., Cook, B. A., Harringa, J., Terpstra, R. L., & Unal, O. (2001). Alloying effects in near-eutectic Sn-Ag-Cu solder alloys for improved microstructural stability. *Journal of Electronic Materials*, *30*(9). https://doi.org/10.1007/s11664-001-0129-5

Andrade, G., Zepon, G., Edalati, K., Mohammadi, A., Ma, Z., Li, H. W., & Floriano, R. (2023). Crystal structure and hydrogen storage properties of AB-type TiZrNbCrFeNi high-

entropy alloy. *International Journal of Hydrogen Energy*, *48*(36). https://doi.org/10.1016/j.ijhydene.2022.12.134

Choi, W. K., & Lee, H. M. (2000). Effect of soldering and aging time on interfacial microstructure and growth of intermetallic compounds between Sn-3.5Ag solder alloy and Cu substrate. *Journal of Electronic Materials*, *29*(10). https://doi.org/10.1007/s11664-000-0014-7

Feather, W. G., Ghorbanpour, S., Savage, D. J., Ardeljan, M., Jahedi, M., McWilliams, B. A., Gupta, N., Xiang, C., Vogel, S. C., & Knezevic, M. (2019). Mechanical response, twinning, and texture evolution of WE43 magnesium-rare earth alloy as a function of strain rate: Experiments and multi-level crystal plasticity modeling. *International Journal of Plasticity*, *120*. https://doi.org/10.1016/j.ijplas.2019.04.019

Galera-Rueda, C., Montero-Sistiaga, M. L., Vanmeensel, K., Godino-Martínez, M., Llorca, J., & Pérez-Prado, M. T. (2021). Icosahedral quasicrystal-enhanced nucleation in Al alloys fabricated by selective laser melting. *Additive Manufacturing*, *44*. https://doi.org/10.1016/j.addma.2021.102053

Kim, M. H., Jung, C. H., Jo, H. H., & Kang, C. S. (2000). The effects of Ti and Sr on the microstructures of Al-11.3 wt.%Si alloys produced by the Ohno continuous casting process. *Metals and Materials International*, *6*(3). https://doi.org/10.1007/BF03028217

Lesyk, D. A., Dzhemelinskyi, V. V., Martinez, S., Mordyuk, B. N., & Lamikiz, A. (2021). Surface Shot Peening Post-processing of Inconel 718 Alloy Parts Printed by Laser Powder Bed Fusion Additive Manufacturing. *Journal of Materials Engineering and Performance*, *30*(9). https://doi.org/10.1007/s11665-021-06103-6

Liang, C., Zou, P., Nairan, A., Zhang, Y., Liu, J., Liu, K., Hu, S., Kang, F., Fan, H. J., & Yang, C. (2020). Exceptional performance of hierarchical Ni-Fe oxyhydroxide@NiFe alloy nanowire array electrocatalysts for large current density water splitting. *Energy and Environmental Science*, *13*(1). https://doi.org/10.1039/c9ee02388g

Moon, K. W., Boettinger, W. J., Kattner, U. R., Biancaniello, F. S., & Handwerker, C. A. (2000). Experimental and thermodynamic assessment of Sn-Ag-Cu solder alloys. *Journal of Electronic Materials*, *29*(10). https://doi.org/10.1007/s11664-000-0003-x

Nishikawa, H., Piao, J. Y., & Takemoto, T. (2006). Interfacial reaction between Sn-0.7Cu (-Ni) solder and Cu substrate. *Journal of Electronic Materials*, *35*(5). https://doi.org/10.1007/BF02692576

Oakwood, T. G., Goodrich, G. M., & Gundlach, R. B. (2002). Role of Gravity Forces on the Directional Solidification of Gray Cast Iron. *Transactions of American Foundry Society*, *110*(02–031).

Parakh, A., Vaidya, M., Kumar, N., Chetty, R., & Murty, B. S. (2021). Effect of crystal structure and grain size on corrosion properties of AlCoCrFeNi high entropy alloy. *Journal of Alloys and Compounds*, *863*. https://doi.org/10.1016/j.jallcom.2020.158056

Ruiz-Esparza-Rodríguez, M. A., Garay-Reyes, C. G., Estrada-Guel, I., Hernández-Rivera, J. L., Cruz-Rivera, J. J., Gutiérrez-Castañeda, E., Gómez-Esparza, C. D., & Martínez-Sánchez, R. (2021). Influence of process control agent and Al concentration on synthesis and phase stability of a mechanically alloyed AlxCoCrFeMnNi high-entropy alloy. *Journal of Alloys and Compounds*, *882*. https://doi.org/10.1016/j.jallcom.2021.160770

Shtender, V. V., Pavlyuk, V. V., Zelinska, O. Y., Nitek, W., Paul-Boncour, V., Dmytriv, G. S., Łasocha, W., & Zavaliy, I. Y. (2020). The Y–Mg–Co ternary system: alloys synthesis, phase diagram at 500 °C and crystal structure of the new compounds. *Journal of Alloys and Compounds*, *812*. https://doi.org/10.1016/j.jallcom.2019.152072

Smith, L. T. W., Su, Y., Xu, S., Hunter, A., & Beyerlein, I. J. (2020). The effect of local chemical ordering on Frank-Read source activation in a refractory multi-principal element alloy. *International Journal of Plasticity*, *134*. https://doi.org/10.1016/j.ijplas.2020.102850

Tong, Q., Ge, J., Rong, M., Li, J., Jiao, J., Zhang, L., & Wang, J. (2022). Thermodynamic Modeling of the Ag-Cu-Sn Ternary System. *Metals*, *12*(10). https://doi.org/10.3390/met12101557

Zhou, J., Huang, D., Fang, Y. L., & Xue, F. (2009). Investigation on properties of Sn-8Zn-3Bi lead-free solder by Nd addition. *Journal of Alloys and Compounds*, *480*(2). https://doi.org/10.1016/j.jallcom.2009.02.064